Adsorption of oxygen molecules on individual single-wall carbon nanotubes

A. Tchernatinsky, S. Desai, G. U. Sumanasekera, C. S. Jayanthi, and S. Y. Wu[a)]
Department of Physics, University of Louisville, Louisville, Kentucky 40292

B. Nagabhirava and B. Alphenaar
Department of Electrical and Computer Engineering, University of Louisville, Louisville, Kentucky 40292

(Received 27 January 2005; accepted 5 December 2005; published online 6 February 2006)

Our study of the adsorption of oxygen molecules on individual semiconductiong single-walled carbon nanotubes at ambient conditions reveals that the adsorption is physisorption, the resistance without O_2 increases by approximately two orders of magnitude as compared to that with O_2, and the sensitive response is due to the pinning of the Fermi level near the top of the valence band of the tube, resulting from impurity states of O_2 appearing above the valence band. © *2006 American Institute of Physics*. [DOI: 10.1063/1.2163008]

I. INTRODUCTION

Interest in gas adsorption by carbon nanotubes at ambient conditions has been spurred by the demonstrations of the potential of single-walled carbon nanotube (SWCNT)-based gas sensors,[1–3] specifically, the establishment of the interdependence between gas adsorption and transport properties of carbon nanotubes (CNTs). In recent years, experimental studies on the adsorption of oxygen molecules by SWNT bundles or mats included the measurements of electrical resistance and thermoelectric power,[2,3] the effect of adsorption of O_2 on the barrier of metal-semiconductor contact,[4,5] and the kinetics of O_2 adsorption and desorption.[6] The picture emerged from these studies relevant to gas sensing indicates that the electrical resistance changes by about 15% between gassing and degassing,[2] that the hole doping of semiconducting single-walled nanotube (*s*-SWNT) in air is by the adsorption of O_2 in the bulk of *s*-SWNTs (Ref. 5) rather than at the contact,[4] and that the adsorption of O_2 has the characteristics of physisorption.[6] Theoretical investigations of the adsorption of O_2 on SWNTs have also been carried out, using spin-unpolarized as well as spin-polarized density-functional theory (DFT) methods.[7–12] Studies of the adsorption of O_2 on small-diameter (8,0) SWNT based on the spin-unpolarized DFT within the local-density approximation (LDA) predicted a weak hybridization between states of O_2 and those of the *s*-SWNT with an estimated charge transfer of $\sim 0.1e$,[7,9] leading to a binding of O_2 at a distance less than 3 Å from the *s*-SWNT. The hole doping of the *s*-SWNT was attributed to the pinning of the Fermi level at the top of the valence band due to the adsorption of O_2. With the O_2 molecule having a triplet ground state, the more realistic calculations based on the spin-polarized gradient-corrected DFT,[8,10,12] on the other hand, yielded a very weak bonding at ~4 Å with no significant charge transfer, indicating that an O_2 molecule in the more stable triplet state is only physisorbed on a *s*-SWNT. For the triplet state of O_2 adsorbed on the (8,0) SWNT, two degenerated $pp\pi^*$ bands were found to split into four bands, with the two unoccupied $pp\pi^*(\downarrow)$ bands rising ~0.35 eV above the top of the valence band at the Γ point,[12] casting some doubt about the hole-doping picture deduced from the unpolarized calculation.

In order to obtain a coherent and consistent picture of the adsorption of O_2 by individual *s*-SWNTs, we have conducted a careful experimental and theoretical investigation of the adsorption of O_2 molecule by individual SWNTs to shed light on the nature of adsorption and its effect on the transport properties of SWNTs. Experimentally, contacts were made to a few very dispersed SWNTs using *e*-beam lithography. The experiment was first conducted under ambient conditions in air (room temperature and atmosphere pressure). The resistance was monitored during each exposure to air and subsequent pumping (10^{-6} Torr). A resistance change of more than one order of magnitude was observed as a result of the adsorption of O_2 by *individual* *s*-SWNTs, in dramatic contrast to a mere 15% change observed for SWNT bundles or mats. Furthermore, the onset of the change in resistance was in minutes. These observations clearly demonstrated the feasibility of constructing *s*-SWNT-based chemical sensors. To be more consistent with the experimental result, we have carried out a study on the adsorption of an O_2 molecule by a larger SWNT than the one considered in previous studies, the (14,0) SWNT, that is closer to the range of diameters in the experiment, using the spin-polarized DFT method. Our calculation using the spin-polarized generalized gradient approximation (GGA) yielded a shallow potential well with depth of the order of ~0.05 eV at ~3.6 Å from the surface of the SWNT, consistent with the picture of physisorption. We have determined the pinning of the Fermi energy due to the impurity level associated with O_2. Our estimate of the resistance based on the result of the (14,0) tube with the adsorption of the O_2 molecule is in excellent agreement with the observed initial resistance in air, indicating the metallization of the *s*-SWNT by hole doping associated with the physisorbed O_2. We have also predicted a change in the resistance about two orders of magnitude between gassing and degassing.

[a)]Author to whom correspondence should be addressed; electronic mail: sywu0001@gwise.louisville.edu

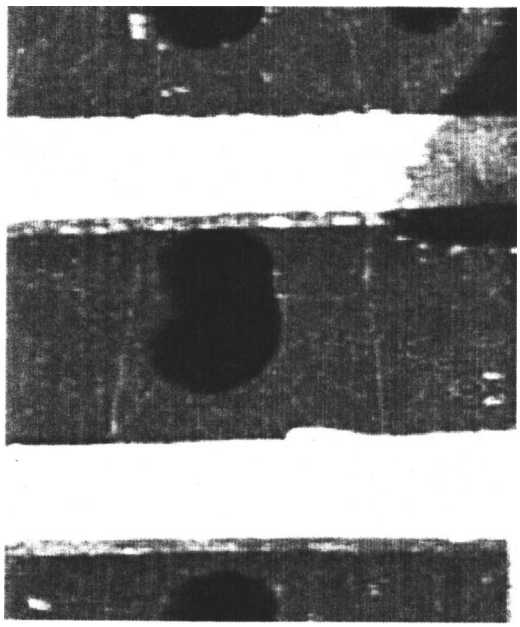

FIG. 1. An AFM image of two SWNTs buried underneath Au/Ti contacts.

II. EXPERIMENTAL RESULTS

Individual SWNTs were synthesized using chemical vapor deposition (CVD) with an Fe catalyst and CH_4 on a SiO_2/Si substrate with prepatterned grid marks. Silicon (100) with a thin oxide layer (0.4 μm) was selected for the growth process. The grid pattern (Au alignment marks) was fabricated on the SiO_2/Si substrate using *e*-beam lithography and etched using a basic oxide etch (BOE). The alignment marks were etched so that they can be seen in atomic force microscopy (AFM) imaging. The preparation of the catalyst solution follows the procedure given in Ref. 13. Fe nanoparticles were dispersed on the substrate from $Fe(NO_3)_3$ propanol solution. After washing with hexane, the substrate was loaded into the CVD reactor and heated to 900 °C in flowing Ar/H_2 [100 SCCM (standard cubic centimeter per minute) of 10% H_2 in Ar]. After reduction at 900 °C for 10 min, methane, the carbon feed, was introduced at a rate of 400 SCCM for 2 min. The sample was cooled in argon. The SWNT samples were imaged using the AFM with reference to the alignment marks in the grid pattern and the Au/Ti contacts were made on the SWNTs using *e*-beam lithography and evaporation. Larger contact pads were deposited on the *e*-beam-defined contacts using optical lithography (see Fig. 1). The device was loaded into a quartz reactor equipped with a turbo-molecular pump capable of evacuating to 10^{-7} Torr for *in situ* studies. The reactor has provisions for gases and chemical vapors.

The experiment was first conducted under ambient conditions (room temperature and atmosphere pressure). The two-probe resistance of the device was measured during the exposure to air and subsequent pumping at room temperature. The resistance was continuously monitored during each exposure and subsequent pumping. Figure 2 shows the time evolution of the two-probe resistance of the device during pumping and subsequent exposure. The data for two cycles are shown. The two-terminal resistance of the as-prepared

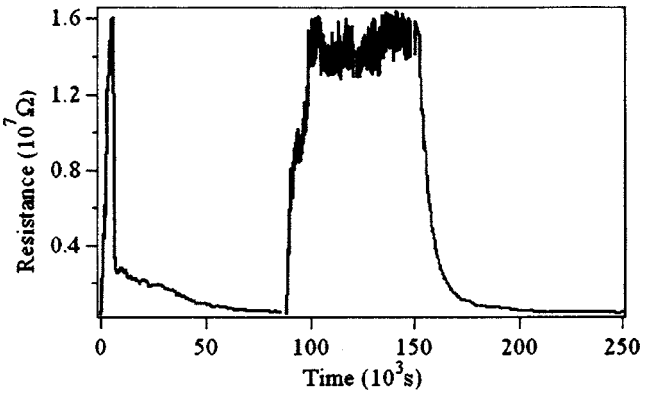

FIG. 2. Two cycles of the time evolution of the two-probe resistance of the sample during pumping and subsequent exposure to air.

device was ~300 kΩ. During pumping ($\leqslant 10^{-6}$ Torr), the resistance started to increase and eventually saturated at a value of ~16 MΩ within a period of ~1 h. This represents a change of the resistance of close to two orders of magnitudes for *individual* SWNTs, a dramatic change in comparison with the ~15% change observed for SWNT bundles or mats.[2] When exposed to air at this point, the resistance started to decrease, initially with an abrupt drop to ~2.5 MΩ within ~15 min. This substantial drop in the resistance within such a short time interval after the exposure to air indicates the sensitivity of the response of individual SWNTs to the absorption of gases in air. The initial drop in resistance was followed by a much slower decrease, saturating at the initial value of ~300 kΩ in ~10 h. A similar behavior was observed in another cycle as shown in Fig. 2. The experimental findings suggest that the fabricated device is most likely composed of *s*-SWNTs and that the findings reflect the response of the transport properties of *s*-SWNT during the exposure to O_2 in air and subsequent pumping. We established the semiconducting nature of our device by measuring the gate voltage dependence of the conductance of the device at room temperature, using a Si substrate as the back gate. We found that when the positive gate voltage is increased, the conductance decreases, while conductance increases when the negative gate voltage is increased. As the conductance of metallic tubes should have little or no gate voltage dependence, and on the other hand, an increasing negative gate voltage adds more holes to *p*-type *s*-SWINTs, thereby increasing the conductance, we conclude that our device consists of only *s*-SWNTs with the *p*-type behavior when exposed to air. This conclusion is consistent with the measurement of a positive thermoelectric power in the case of the adsorption of O_2 molecules by SWNT bundles reported in Ref. 3, which indicates a *p*-type behavior for *s*-SWNTs with the adsorption of O_2 molecules.

In Fig. 3 we show the gate voltage (V_g) dependence of I_{ds} (for V_{ds}=300 mV) before and after the removal of air. The degenerately doped Si substrate was used as the back gate. The data were collected after the resistance reached the saturation values for both increasing and decreasing gate voltages. The I_{ds} vs V_g characteristics clearly show that the air-doped SWNTs (corresponding to the lowest resistance value) behave as a *p*-type semiconductor, i.e., they are on for a

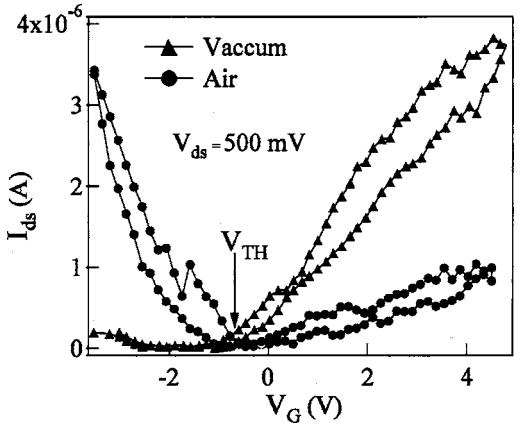

FIG. 3. Gate voltage dependence of I_{ds} before and after removal of air. $V_{ds}=300$ mV. The data were collected after the resistance values reached the saturation values for both increasing and decreasing gate voltages.

negative gate bias. It shows some ambipolar properties as the device is not completely off for a positive gate bias, typical for most SWNT-based field-effect transistors (FETs). After pumping, its electronic character changes to *n* type (corresponding to the highest resistance value) as it exhibits a complete off state for a positive gate bias. The hysteresis observed in I_{ds} for decreasing and increasing gate voltages has been observed in most of the SWNT-based FETs and interpreted as due to trapped electrons. Most interestingly, the threshold voltage (marked in Fig. 3 by a downward arrow) for both *p*- and *n*-type devices is essentially the same. This is a conclusive indication that there is no charge transfer between the adsorbed O_2 molecules and the *s*-SWNT, which is confirmed by our theoretical calculations, to be presented in Sec. III.

III. THEORETICAL ANALYSIS

To shed light on the physics underlying the change in the transport properties during the adsorption and desorption of O_2 molecules by *s*-SWNTs, we carried out a detailed study of the adsorption of an O_2 molecule on a (14,0) *s*-SWNT, using spin-polarized LDA as well as spin-polarized GGA DFT methods in the Vienna *ab initio* simulation package (VASP).[14–16] We chose to use the (14,0) SWNT as the benchmark because its diameter ($d=1.10$ nm) is close to the range of diameters of typical SWNTs and a recent DFT calculation has established the $1/d$ dependence of the energy gap of *s*-SWNTs to be valid only for $d \geqslant 1.0$ nm.[17] In our calculation, we used a supercell of size $26\times26\times8.54$ Å to cut down the potential image effect between SWNTs. Along the axial direction of the SWNT, this supercell consists of two SWNT unit cells so that the calculation reflects well the situation of the physisorption of individual O_2 molecules. Vanderbilt's ultrasoft pseudopotential[18,19] and the Perdew-Zunger functional,[20] with the GGA correction of Perdew *et al.*,[21] were used for the self-consistent spin-polarized solution. The energy cut off was set at 700 eV. Monkhorst-Pack scheme with $1\times1\times11$ *k*-point mesh was used for sampling the Brillouin zone. Full optimization of the structural configuration of SWNT+O_2 and the lattice constants were carried out using the conjugate gradient method with the energy convergence of 10^{-5} eV and forces $\leqslant 10^{-2}$ eV/Å.

Our calculations, using spin-unrestricted LDA as well as GGA, confirmed that the triplet O_2 state has a lower energy as compared with the singlet state. Before using the VASP code to investigate the benchmark case of the (14,0) *s*-SWNT+O_2, we applied in to the case of the (8,0) *s*-SWNT+O_2 with O_2 near the *T* site.[12] The optimization yields a result in excellent agreement with the corresponding result in Ref. 12 [see Fig. 5(g) in Ref. 12]. Having established the validity of the VASP code, we carried out optimizations of the adsorption of O_2 on the (14,0) *s*-SWNT with spin-polarized methods (LDA and GGA). We found the binding to be the strongest for the triplet O_2 molecule near the top of two adjacent zigzag bonds (*T* site), with the molecular axis perpendicular to the axial direction of the SWNT (see Fig. 4, left panel). The relaxed bonding geometries (bond length and equilibrium orientation of O_2) from both methods are almost the same except for the equilibrium distance from O_2 to the surfaces of the (14,0) SWNT. Figure 4 (right panel) shows a weak potential well of depth ~0.1 eV at a distance of ~3.0 Å for the LDA result and a very shallow well of ~0.03 eV at a distance of ~3.5 Å for the GGA result. These results are consistent with the scenario of physisorption. For physisorption characterized by weak interactions, LDA tends to overestimate the binding and underestimate the equilibrium distance, while GGA tends to underestimate the binding. From our result, one can conclude that the physisorption of O_2 on the (14,0) *s*-SWNT is characterized by a potential well of depth between 0.03 and 0.1 eV and an equilibrium distance between 3.0 and 3.5 Å.

Figure 5 shows the band structures in the vicinity of the energy gap of relaxed configurations of the adsorption of triplet O_2 on the surface of the (14,0) *s*-SWNT obtained by

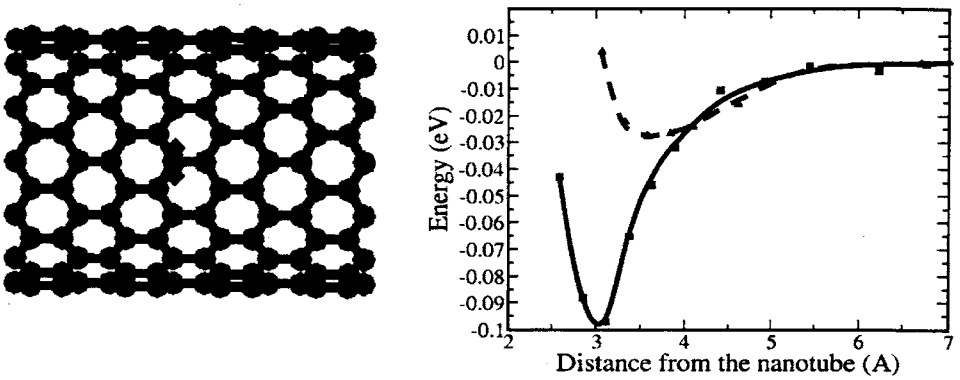

FIG. 4. The binding of a triplet O_2 near the top of two adjacent zigzag bonds. Left panel: The equilibrium configuration. Right panel: Energy vs distance curves (dotted curve, GGA result; solid curve, LDA result).

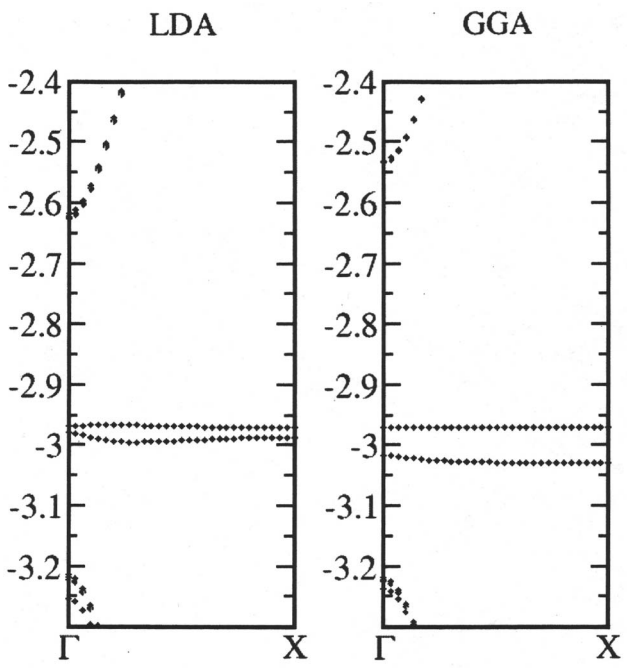

FIG. 5. Band structures corresponding to the equilibrium configurations. Left panel: LDA result; right panel: GGA result.

LDA and GGA, respectively. The energy gap obtained by the GGA calculation is ~0.69 eV, while that by LDA is ~0.60 eV. We have also checked the band structure for the pristine (14,0) *s*-SWNT using the same methods. We found the same values for the gap and no difference in the band structures as compared with those for the case of $(14,0)+O_2$ by the respective methods. Furthermore, the unoccupied oxygen $pp\pi^*(\downarrow)$ bands were found to appear within the gap of the *s*-SWNT almost dispersionless in both calculations. These results present an unambiguous indication of a very weak interaction between the oxygen molecule and the (14,0) *s*-SWNT, reinforcing the scenario of the physisorption. In this sense, our calculations have essentially established the placement of the empty impurity bands within the gap of the *s*-SWNT. Specifically, for the GGA calculation, the lower $pp\pi^*(\downarrow)$ band is ~0.20 eV above the top of the valence band, while that for the LDA is ~0.24 eV above the top of the valence band. To summarize, our study indicates no charge transfer between O_2 and the (14,0) *s*-SWNT. The effect of the presence of the oxygen impurity bands is to pin the Fermi level to the vicinity of the top of the valence band.

The conductance for the pristine *s*-SWNT and that for the *s*-SWNT with O_2 under ambient conditions can be estimated according to

$$G = \frac{2e^2}{h}\int_{-\infty}^{\infty} T(E)\left(-\frac{\partial f}{\partial E}\right)dE \approx G_0\left(\frac{2}{1+e^{\Delta/2kT}}\right), \qquad (1)$$

where $T(E)$ is the transmission coefficient as a function of E and may be approximated by 2 in the vicinity of the Fermi energy for SWNTs, $f(E)$ is the Fermi distribution function, $G_0=4e^2/h$ is the quantum conductance, and Δ is the energy gap. Using Eq. (1) based on the energy gap with or without O_2 obtained by LDA as well as GGA, we have calculated the resistances of the (14,0) *s*-SWNT with or without O_2 at room temperature. The results are shown in Table I. It can be seen that the GGA method yields a value of ~400 kΩ for the resistance with O_2, in very good agreement with the experimental result, while the LDA method gives rise to a value of ~680 kΩ. For the (14,0) *s*-SWNT, the GGA method leads to a resistance increase by a factor of $\sim 1.33\times 10^4$ between the resistance of the *s*-SWNT without O_2 and that with O_2, while the LDA leads to an increase in resistance by a factor of 1.08×10^3. This resistance change can be attributed to the pinning of the Fermi level to the vicinity of the valence band due to the presence of the empty oxygen bands. Since the diameter of a typical SWNT is ~1.40 nm and the gap follows a $1/d$ dependence on the diameter for $d \geqslant 1$ nm, we estimated the energy gap of the typical *s*-SWNT using the calculated gap of the (14,0) SWNT ($d=1.09$ nm) according to $\Delta_{adj}=\Delta\times 1.09/1.4$. Using Δ_{adj}, we obtained a resistance increase by a factor of 82 for the LDA result and 652 for the GGA result, consistent with the experimental result.

IV. DISCUSSION

Our experimental study and theoretical analysis clearly lead to the following conclusion concerning the adsorption and desorption of O_2 molecules on *s*-SWNTs: (i) The resistance change between the desorption and absorption of O_2 molecules by an *individual* *s*-SWNT is approximately two orders of magnitude. The response of individual *s*-SWNTs to the exposure to O_2 molecules is therefore far more sensitive as compared with the response of SWNT bundles or mats studied previously. (ii) The adsorption of O_2 molecules on *s*-SWNTs is unequivocally physisorption. There is no charge transfer between the O_2 molecules and the *s*-SWNT. (iii) The sensitive response of *s*-SWNTs to the adsorption of O_2 molecules is due to the pinning of the Fermi level near the top of the valence band.

TABLE I. Resistances of the (14,0) SWNT without (w/o) and with O_2 at room temperature, and their ratio, calculated by spin-polarized LDA and GGA, respectively. Also shown are the adjusted resistances corresponding to a *s*-SWNT (without O_2) with a diameter of 1.40 nm.

	R w/o O_2 (kΩ)	R with O_2 (kΩ)	Ratio	R w/o O_2(kΩ) adjusted	Ratio adjusted
LDA	7.4×10^5	6.8×10^2	1.08×10^3	5.6×10^4	8.20×10^1
GGA	5.2×10^6	4.0×10^2	1.33×10^4	2.6×10^5	6.52×10^2

ACKNOWLEDGMENTS

We would like to acknowledge the support by the NSF (DMR-0112824 and ECS-0224114) and the DOE (DE-FG02-00ER4582).

[1]J. Kong, N. R. Franklin, C. Zhou, M. G. Chapline, S. Peng, K. Cho, and H. Dai Science **287**, 622 (2000).
[2]P. G. Collins, K. Bradley, M. Ishigami, and A. Zettl, Science **287**, 1801 (2000).
[3]C. K. W. Adu, G. U. Sumanasekera, B. K. Pradham, H. E. Romero, and P. C. Eklund, Chem. Phys. Lett. **337**, 31 (2001).
[4]V. Derycke, R. Martel, J. Appenzeller, and Ph. Avouris, Appl. Phys. Lett. **80**, 2773 (2002).
[5]M. Shim and G. P. Siddons, Appl. Phys. Lett. **83**, 3564 (2003).
[6]H. Ulbricht, G. Moos, and T. Hertel, Phys. Rev. B **66**, 075404 (2002).
[7]S.-H. Jhi, S. G. Louie, and M. L. Cohen, Phys. Rev. Lett. **85**, 1710 (2000).
[8]D. C. Sorescu, K. D. Jordan, and Ph. Avouris, J. Phys. Chem. B **105**, 11227 (2001).
[9]J. Zhao, A. Buldum, J. Han, and J. P. Lu, Nanotechnology **13**, 195 (2002).
[10]P. Giannozzi, R. Car, and G. J. Scoles, Chem. Phys. **118**, 1003 (2003).
[11]M. Grujicic, G. Cao, and R. Singh, Appl. Surf. Sci. **211**, 166 (2003).
[12]S. Dag, O. Gülseren, T. Yildirim, and S. Ciraci, Phys. Rev. B **67**, 165424 (2003).
[13]J. H. Hafner, C. L. Cheung, Th. Oosterkamp, and C. M. Lieber, J. Phys. Chem. B **105**, 743 (2001).
[14]G. Kresse and J. Hafner, Phys. Rev. B **48**, 13115 (1993).
[15]G. Kresse and J. Furthmuller, Phys. Rev. B **54**, 11169 (1996).
[16]G. Kresse and J. Furthmuller, Comput. Mater. Sci. **6**, 15 (1996).
[17]V. Zólyomi and J. Kürti, Phys. Rev. B **70**, 085403 (2004).
[18]D. Vanderbilt, Phys. Rev. B **41**, 7892 (1990).
[19]G. Kresse and J. Hafner, J. Phys.: Condens. Matter **6**, 8245 (1994).
[20]J. P. Perdew and A. Zunger, Phys. Rev. B **23**, 5048 (1981).
[21]J. P. Perdew, J. A. Chevary, S. H. Vosko, K. A. Jackson, R. D. Rederson, D. J. Singh, and C. Fiolhais, Phys. Rev. B **46**, 6671 (1992).